Supporting Information

Photoinduced metastable-charging *d*-orbital electrons of Re centers enhances interfacial charge migration behaviors for efficient coupling conversion

Xiang Li[a], Guiyang Yu[a,*] , Ruihong Sun[a], Ke Gong[b], Jinghao Zhu[a], Debao Wang[a]

[a] Key Laboratory of Optic-electric Sensing and Analytical Chemistry for Life Science (MOE), College of Chemistry and Molecular Engineering, Qingdao University of Science and Technology, Qingdao, 266042, PR China.

[b] School of Materials Science and Engineering, Ocean University of China, Qingdao 266100, China

Corresponding Email: yugy3413@qust.edu.cn

Contents

benzaldehyde by HPLC analysis.

Fig. S10. HPLC analysis of (a) standard products and (b) intermediate products in the preliminary reduction process of oxidative coupling reaction of benzylamine.

Fig. S11. (a) Photocatalytic oxidative coupling of benzylamine and (b) bar chart of conversion rate for 6 h over ZIS, 10% ReS_2/ZIS and 10% ReS_2/ZIS-Mix samples.

Fig. S12. XRD patterns of 10% ReS_2/ZIS sample before and after reaction.

Fig. S13. (a) Re 4f, (b) In 3d, and (c) Zn 2p XPS spectra of 10% ReS_2/ZIS sample before and after reaction.

Fig. S14. (a) Photocatalytic oxidative coupling of various benzylamine derivatives benzylamine and (b) bar chart of conversion rate for 6 h over 10% ReS_2/ZIS sample.

Fig. S15. The cyclic voltammogram of benzylamine.

Fig. S16. EPR spectra of ZIS and 10%ReS_2/ZIS samples in the presence of DMPO under benzylamine-acetonitrile reaction solution.

Fig. S17. ^{1}H NMR of intermediate products in the reaction process of photocatalytic oxidative coupling of amines.

Fig. S18. UV-vis absorption spectra of reaction system (benzylamine oxidation) with or without 10%ReS_2/ZIS photocatalyst after adding DPD and POD.

Table S1. The element content of ZIS and ReS_2/ZIS according to ICP result.

Table S2. Fitting parameters of Re 4f XPS spectra for Ar^+-etched ReS_2/ZIS sample before and after light illustration.

Table S3. The measured conductivity (σ), carrier mobility (μ), carrier concentration (c), and I/V using electrochemical characterization.

3. Reference

1. Experimental Section

1.1 Preparation of $ZnIn_2S_4$ (ZIS)

Typically, 136 mg of $ZnCl_2$, 586 mg of $InCl_3 \cdot 4H_2O$, and 751 mg of thioacetamide (TAA) were dissolved by sonication in 30 mL deionized water and stirred for one hour. Then the mixture was transferred into a 50 mL Teflon-lined stainless-steel autoclave and heated to 180 ºC for 12 h. After nature cooling, the $ZnIn_2S_4$ product was collected by centrifugation and subsequently washed by deionized water and ethanol for three times, and finally vacuum-dried at 60 ºC.

1.2 Material Characterization

The crystallite property was examined using the X-ray diffraction (XRD) characterization containing a Rigaku X-ray diffractometer of Cu Kα radiation (λ=1.5418 Å, 50 kV, 200 mA). The scanning rate is 10 º/min from 10º to 70º. The morphology and holey property were investigated using JEOL JSM-6700F field-emission scanning electronic microscope (SEM) and JEM 2100 transmission electron microscopy (TEM) with the accelerating voltage of 10 kV and 200 kV, respectively. Hitachi UV-3900 spectrophotometer was used to analyze the UV-vis diffused reflectance spectra (DRS) of the samples, in which $BaSO_4$ acts as blank reference. The surface areas and pore distribution were determined by N_2 adsorption/desorption isotherms and Brunauer-Emmett-Teller (BET) method. The sample was heated to 150 ºC maintaining 5 h in order to evacuate any moisture and solvent molecules inner the pore. The elemental analysis was carried out on an inductively coupled plasma mass spectrometry (ICP-MS, PerkinElmer, ELAN9000).

1.3 Photoelectrochemical measurements

The transient photocurrent responses, and electrochemical impedance spectroscopy (EIS) were investigated on a CHI760D electrochemical workstation (Shanghai Chenhua Instrument Corp., China) in a conventional three-electrode system composed of a Pt sheet counter electrode, a saturated Ag/AgCl as reference electrode and a working electrode. Firstly, the working electrode was fabricated by spin-coating ethanol suspensions onto pre-cleaned FTO glass (1×1 cm^{-2}) surface. Typically, 5 mg sample was dispersed evenly in 2 mL ethanol with 10 μL Nafion solution, followed by ultrasonic treatment for 1 h to form homogeneous solution. The above solution was dipped (40 μL) and spin-coated (200 $r \cdot min^{-1}$, 10 s) onto the pre-cleaned FTO conductive glass surface, and then dried at room temperature. The above coating process was repeated ten times. Moreover, 0.5 M Na_2SO_4 aqueous solution was used as supporting electrolyte. A 300 W Xe lamp equipped with a 420 nm optical cutoff filter was used at light source.

1.4 Density-functional-theory (DFT) calculations

All calculations are performed with the Vienna Ab-initio Simulation Package (VASP) in the framework of density functional theory (DFT).[1,2] The projector augmented wave (PAW) method [3,4] is used to describe the electrons-ionic interactions and the generalized gradient approximation (GGA) together with the Perdew-Burke-Ernzerhof (PBE)[5] is employed to describe all exchange and correlation effects. Grimmes's dispersion correction D3 is used to account for the vdW interaction.[6,7] A cutoff energy of 400 eV is used to ensure the precision of calculations. Brillouin zone

is sampled using the Monkhorst–Pack by a 6×6×1 k-point grid for $ZnIn_2S_4$ semiconductor and 5×5×1 k-point mesh was used for one-layer ReS_2. Gaussian smearing with a width of 50 meV was used for the occupation of electronic levels. To simulate the $ReS_2/ZnIn_2S_4$ composites, ReS_2 were put on a (2 × 2) stoichiometric $ZnIn_2S_4$ surface slab. Convergence criteria are set to be 10^{-5} eV for energy and 0.03 eV/Å for the forces and the interaction between adjacent layers was prevented by setting up a 1.5 nm vacuum layer. To get the exact DOS results, we increased the number of k-point and use 9 × 9 × 1 k-point grid.

1.5 Calculation of Fermi level from UPS spectra

In the UPS spectra, it is well known that the position of vacuum level (E_{vac}) is located 21.22 eV above the cutoff energy (E_{cutoff}) of the spectrum. Using ZIS as example, Fig. 3a shows the E_{cutoff} of ZIS is 17.58 eV. Hence the E_f is calculated to be −3.64 eV based on the formula of E_{cutoff}−21.22 (vs. vacuum). According to the difference between vacuum energy level and NHE level, the E_f of ZIS is determined to be −0.86 V (−4.5−(−3.64)= −0.86 V) (vs. NHE).

1.6 Calculation formula for k_{IR} and η_{int}

Based on the average lifetime of ZIS, ReS_2/ZIS, and ReS_2/ZIS-Mix, the injection rate is determined by the following formula[8]:

$$k_{IR} = \frac{1}{\tau_{ave}(ReS_2/ZIS)} - \frac{1}{\tau_{ave}(ZIS)} \quad [1]$$

$$k_{IR} = \frac{1}{\tau_{ave}(ReS_2/ZCS - Mix)} - \frac{1}{\tau_{ave}(ZIS)} \quad [2]$$

The efficiency of electron injection (η_{int}) into ReS_2, as a more important parameter

for activity, is acquired as[9]:

$$\eta_{inj} = 1 - \frac{\tau_{ave}\left(ReS_2/ZIS\right)}{\tau_{ave}(ZIS)} \quad [3]$$

$$\eta_{inj} = 1 - \frac{\tau_{ave}\left(ReS_2/ZCS - Mix\right)}{\tau_{ave}(ZIS)} \quad [4]$$

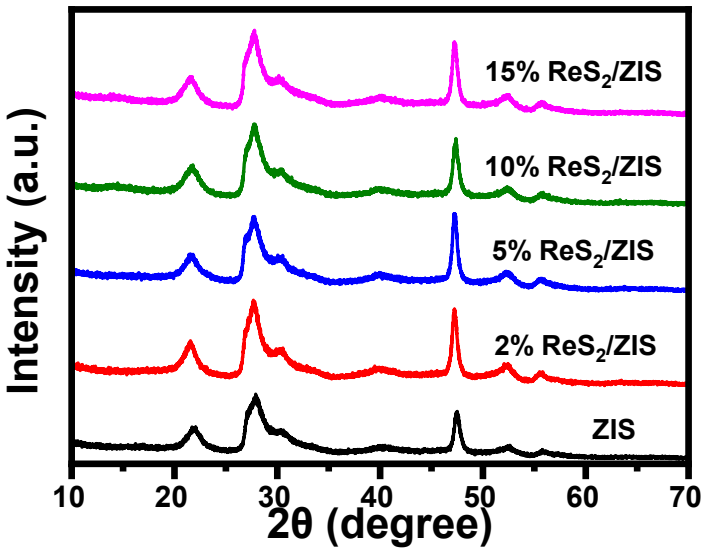

Fig. S1. XRD patterns of ZIS and various ReS_2/ZIS samples.

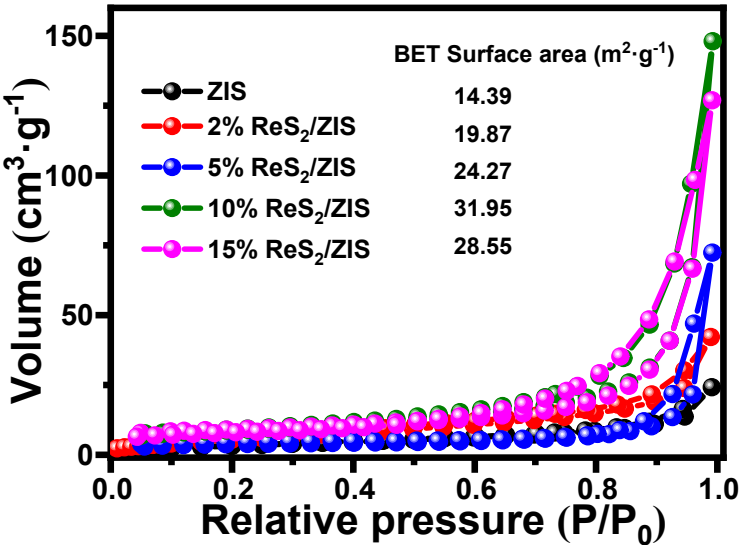

Fig. S2. N_2 absorption-desorption isotherms of ZIS and ReS_2/ZIS samples.

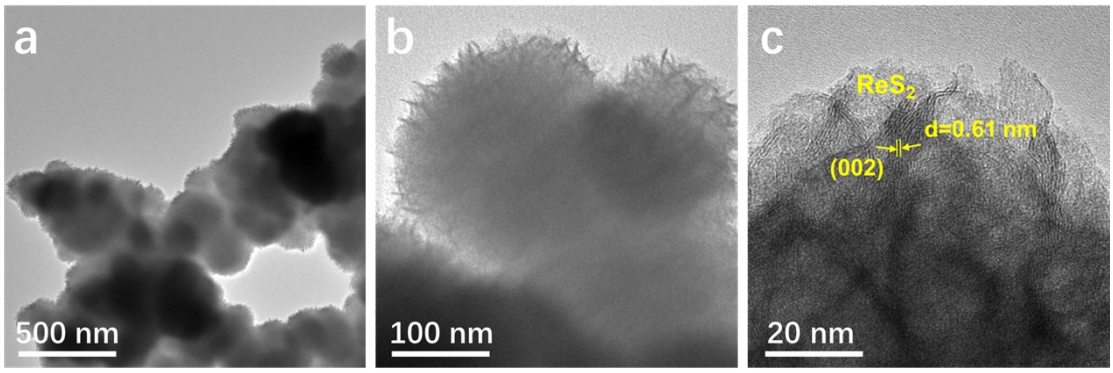

Fig. S3. (a and b) TEM images and (c) HRTEM image of pure ReS_2.

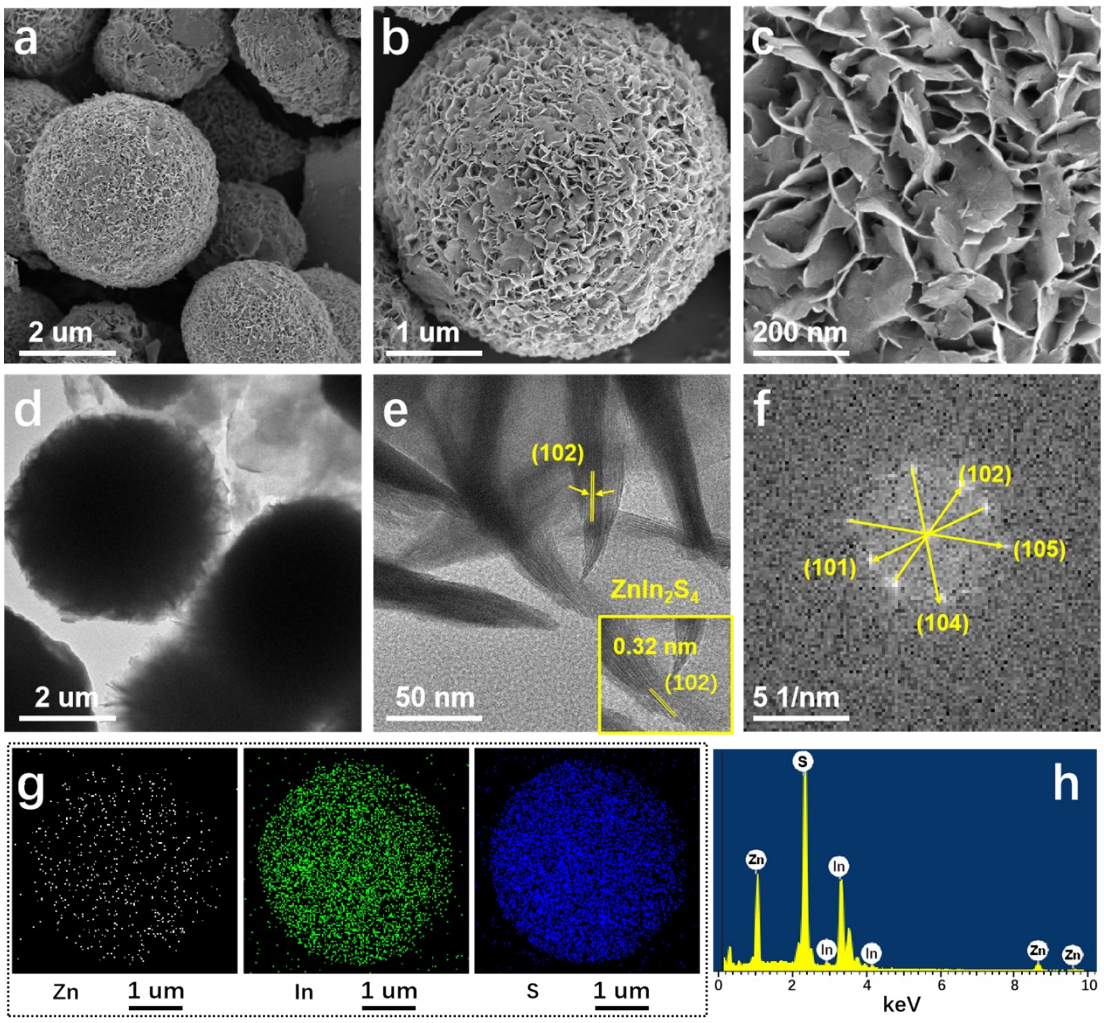

Fig. S4. (a-c) SEM images, (d and e) TEM images, (f) SAED image, (g) element mapping image for Zn, In, and S elements, (h) EDX image of $ZnIn_2S_4$ sample.

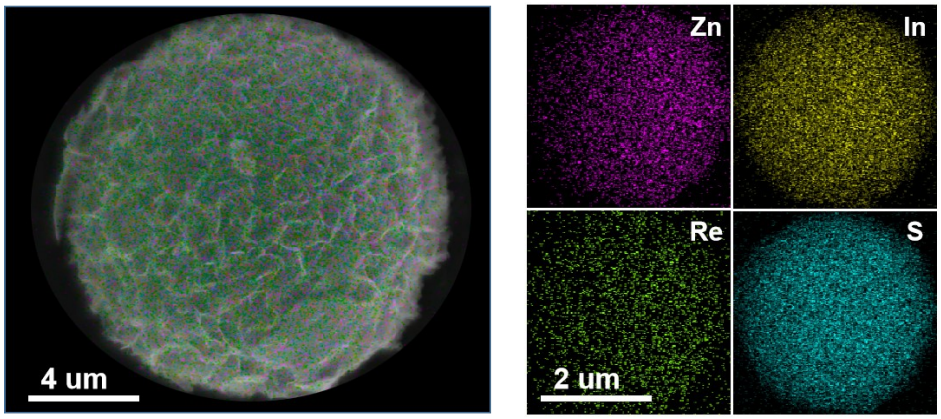

Fig. S5. EDX mapping images for Zn, In, Re, and S elements of 10% ReS_2/ZIS sample.

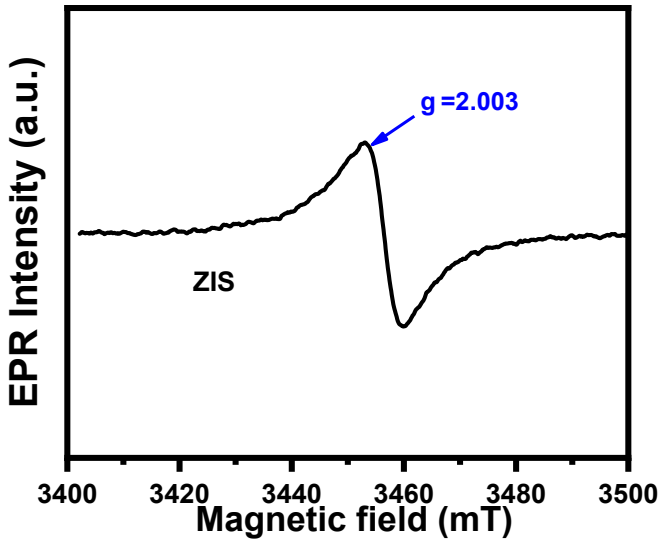

Fig. S6. EPR spectra of pristine ZIS.

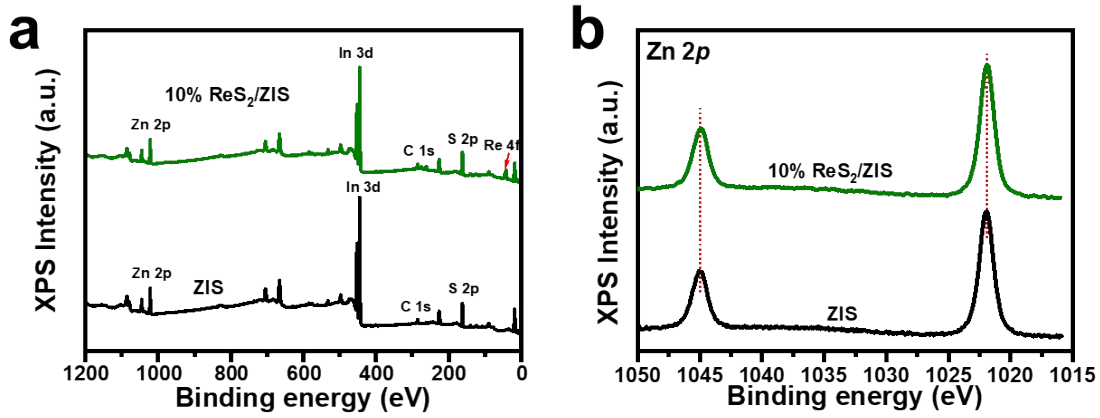

Fig. S7. (a) XPS survey spectra and (b) Zn 2p XPS spectra of ZIS and 10% ReS_2/ZIS samples.

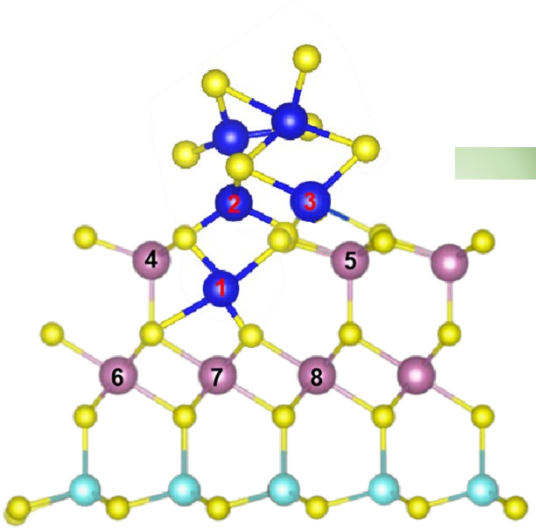

Atom number	Bader Charge transfer number
Re-1	-0.57457
Re-2	-0.60794
Re-3	-0.55518
In-4	0.86931
In-5	0.85017
In-6	0.81627
In-7	0.83378
In-8	0.78940

Fig. S8. Structural model for ReS_2/ZIS and the Bader charge transfer number of neighboring atoms.

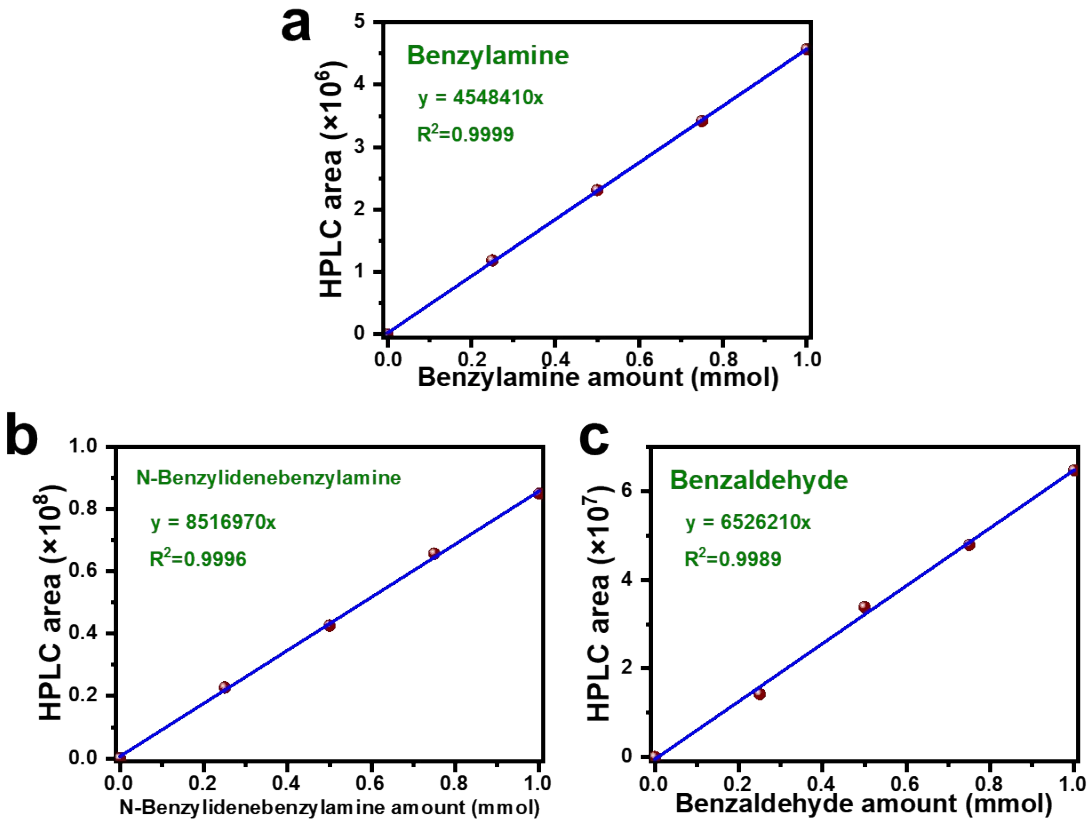

Fig. S9. Standard curves of (a) benzylamine, (b) N-benzylidenebenzylamine and (c) benzaldehyde by HPLC analysis.

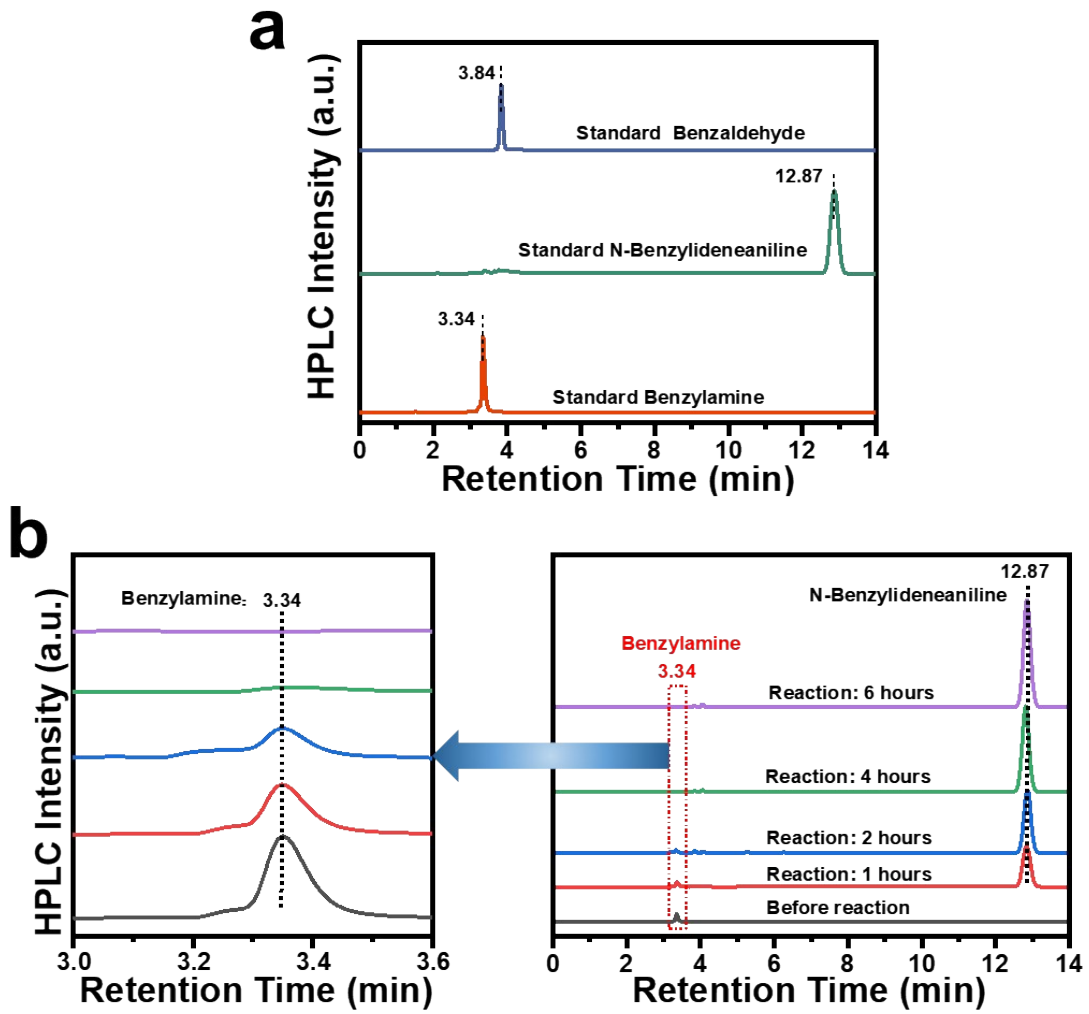

Fig. S10. HPLC analysis of (a) standard products and (b) intermediate products in the preliminary reduction process of oxidative coupling reaction of benzylamine.

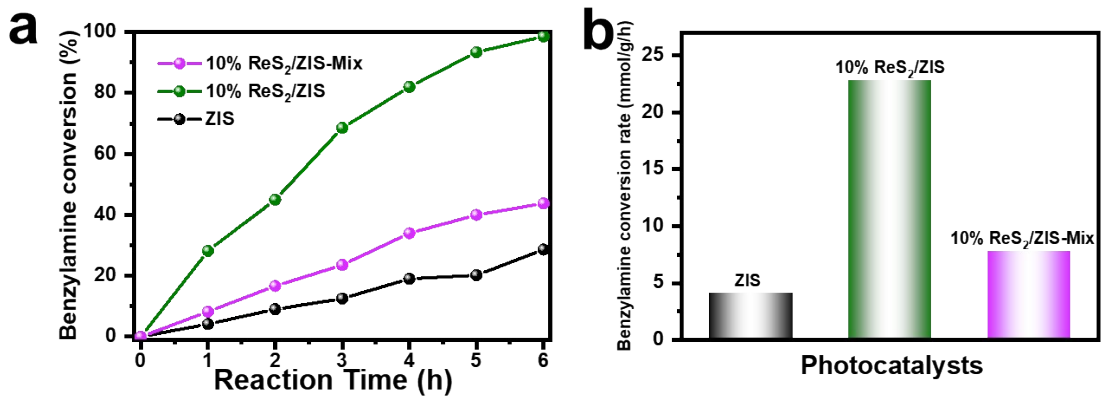

Fig. S11. (a) Photocatalytic oxidative coupling of benzylamine and (b) bar chart of conversion rate for 6 h over ZIS, 10% ReS_2/ZIS and 10% ReS_2/ZIS-Mix samples.

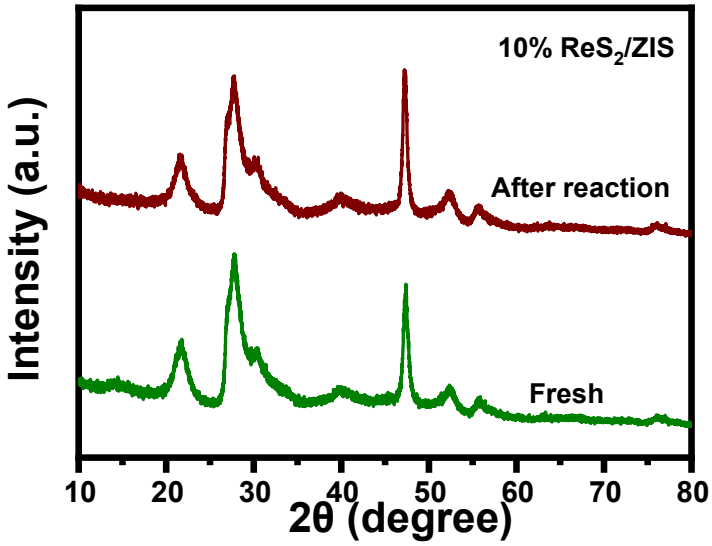

Fig. S12. XRD patterns of 10% ReS_2/ZIS sample before and after reaction.

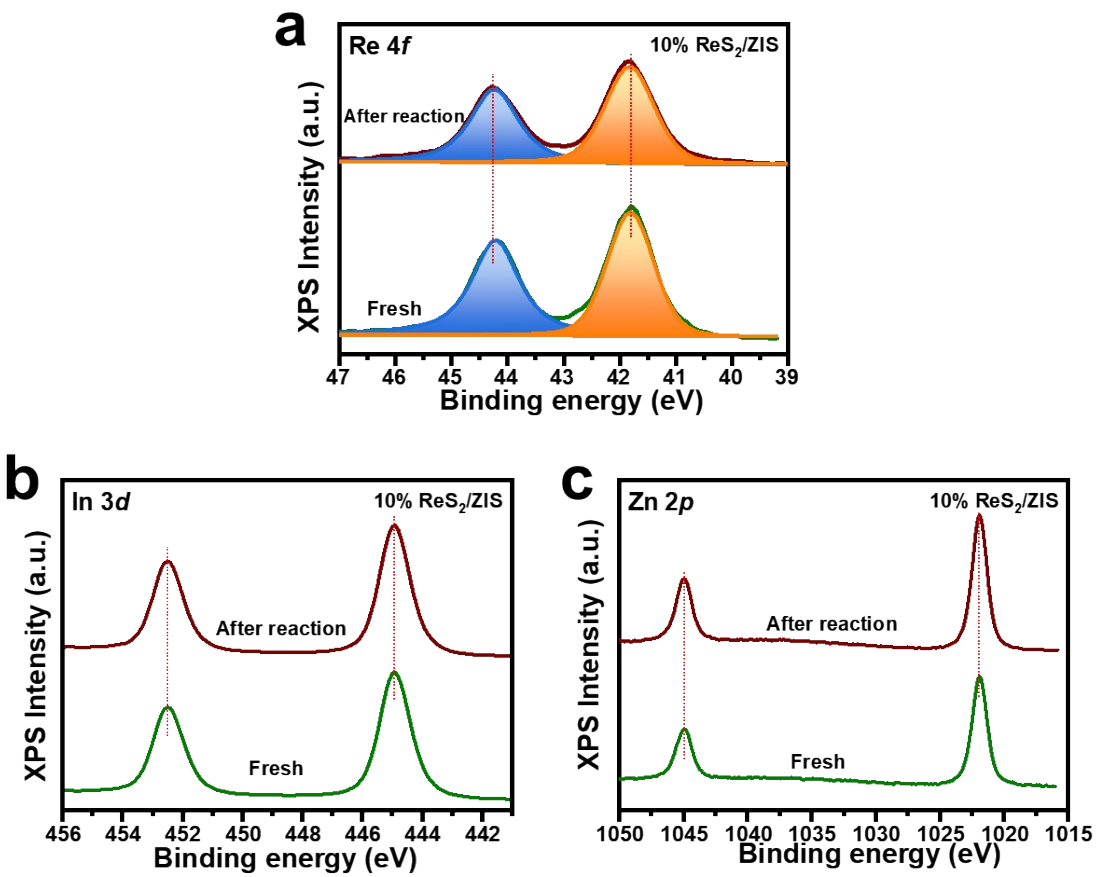

Fig. S13. (a) Re 4f, (b) In 3d, and (c) Zn 2p XPS spectra of 10% ReS_2/ZIS sample before and after reaction.

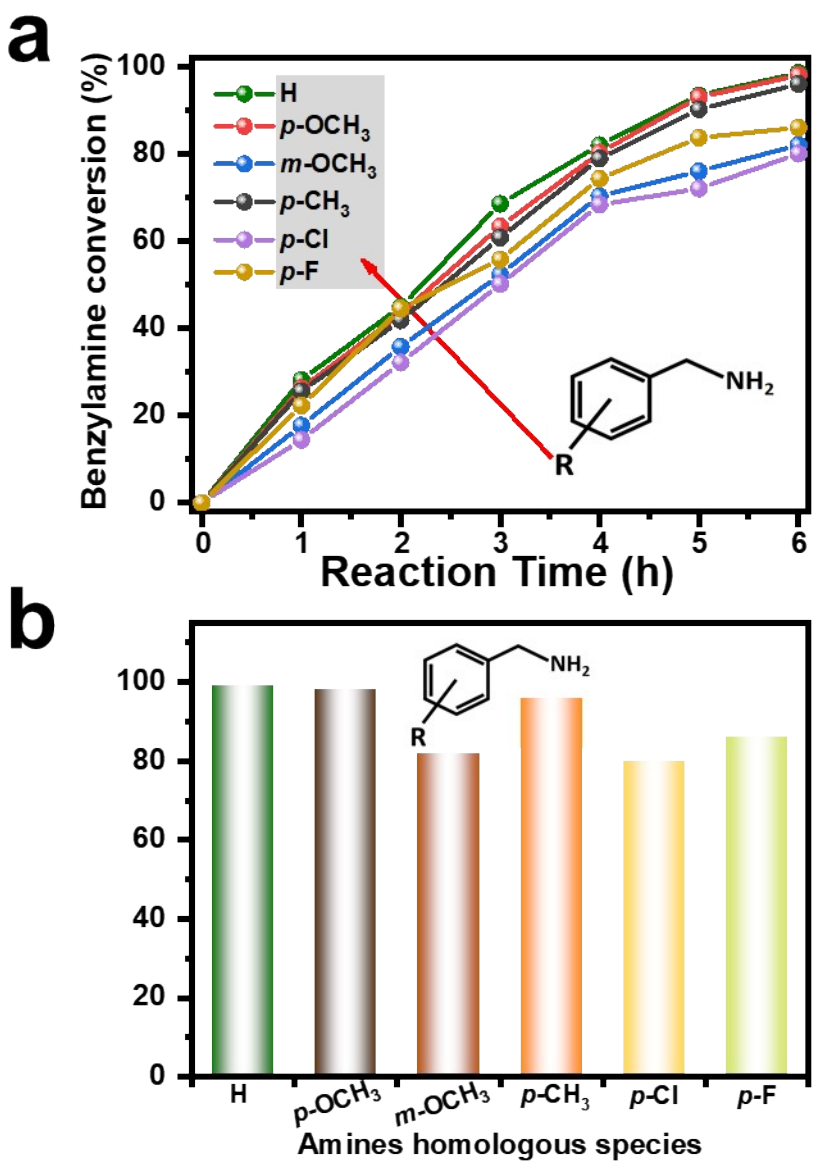

Fig. S14. (a) Photocatalytic oxidative coupling of various benzylamine derivatives benzylamine and (b) bar chart of conversion rate for 6 h over 10% ReS_2/ZIS sample.

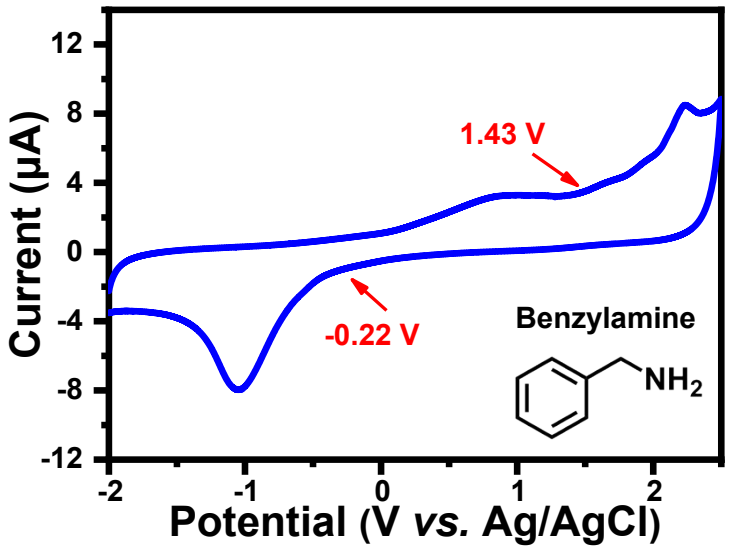

Fig. S15. The cyclic voltammogram of benzylamine.

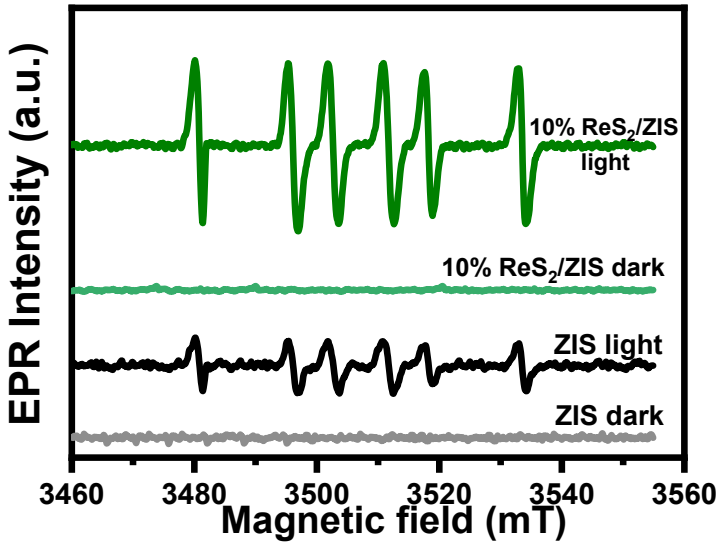

Fig. S16. EPR spectra of ZIS and 10%ReS_2/ZIS samples in the presence of DMPO under benzylamine-acetonitrile reaction solution.

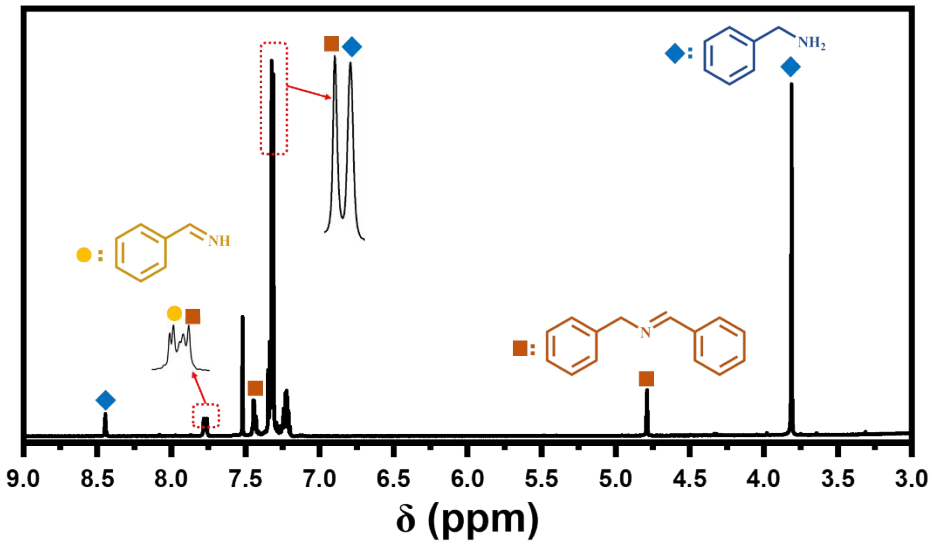

Fig. S17. ^{1}H NMR of intermediate products in the reaction process of photocatalytic oxidative coupling of amines.

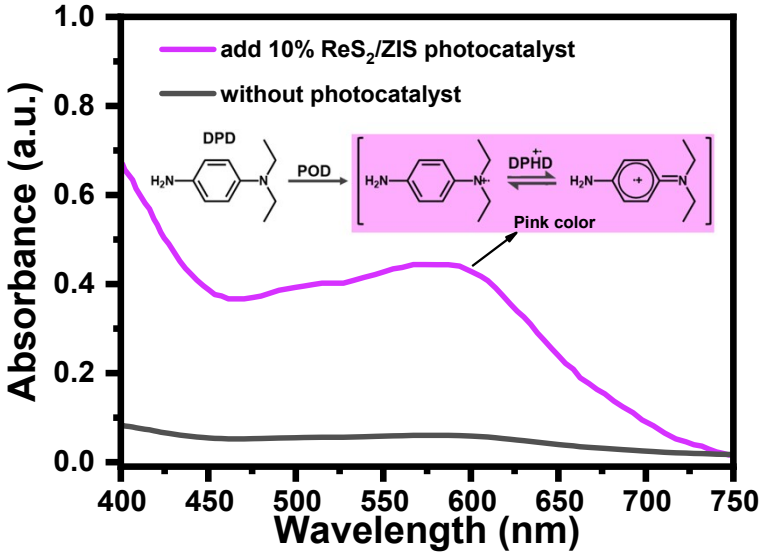

Fig. S18. UV-vis absorption spectra of reaction system (benzylamine oxidation) with or without 10%ReS_2/ZIS photocatalyst after adding DPD and POD.

Table S1. The element content of ZIS and ReS_2/ZIS according to ICP result.

Sample	Zn (wt%)	In (wt%)	Re (wt%)
ZIS	15.4619	53.9258	——
2% ReS_2/ZIS	15.1601	53.2708	1.4437
5% ReS_2/ZIS	14.7148	51.6637	3.5872
10% ReS_2/ZIS	13.9619	49.0202	7.2112
15% ReS_2/ZIS	13.3157	46.7513	10.3226

Table S2. Fitting parameters of Re 4f XPS spectra for Ar^+-etched ReS_2/ZIS sample before and after light illustration.

Condition	Fitting parameter	Re^{4+} species		$Re^{(4-\delta)+}$ species	
		Peak I	Peak II	Peak III	Peak IV
Ar^+-etched ReS_2/ZIS before light illumination	Peak position (eV)	44.22	41.61	43.63	41.21
	FWHM	1	1	1.22	0.92
	Peak area	1388	1505	1013	883
	Area percentage	28.98	31.43	21.15	18.44
	(%)	60.41		39.59	
Ar^+-etched ReS_2/ZIS after light illumination	Peak position (eV)	44.22	41.61	43.73	41.23
	FWHM	1	1	1.22	0.92
	Peak area	1150	1441	1439	820
	Area percentage	23.71	29.71	29.67	16.91
	(%)	53.42		46.58	

Table S3. The measured conductivity (σ), carrier mobility (μ), carrier concentration (c), and I/V using electrochemical characterization.

Sample	I/V (μA/V)	σ ($S \cdot m^{-1}$)	c (cm^{-3})	μ ($cm^2 \cdot V^{-1} \cdot s^{-1}$)[1]
ZIS	0.181	0.006	3.18×10^{15}	0.117
10% ReS_2/ZIS-Mix	0.697	0.023	4.18×10^{15}	0.343
10% ReS_2/ZIS	2.106	0.069	5.96×10^{15}	0.726

[1.] The carrier mobility (μ) of ZIS, 10% ReS_2/ZIS-Mix and 10% ReS_2/ZIS samples is calculated according to the following equations:[10]

$$\sigma = \frac{dI}{(2n-1)LhV} \quad [5]$$

$$\sigma = cq\mu \quad [6]$$

Where d is the interelectrode spacing (75 μm), I is the current, n is the number of electrode digits (the interdigitated array electrode in our measurement is composed of n =10 pairs of ITO electrode digits deposited onto a glass substrate), L is the overlapping length of the electrodes (6000 μm), h is the film thickness (20 nm), c is the charge carrier concentration, and q stands for elementary charge (1.6×10^{-19} C).

Table S4. Time constant τ of fluorescence decay curves of ZIS, 10% ReS_2/ZIS-Mix and 10% ReS_2/ZIS.

Samples	τ_1 (ns)	A_1 %	τ_2 (ns)	A_2%	τ_3 (ns)	A_3%	τ_{ave} (ns)
ZIS	0.8312	18.11	4.5452	45.83	40.0107	36.06	35.2227
10% ReS_2/ZIS-Mix	0.7927	36.95	3.8388	38.51	38.9262	24.54	33.3591
10% ReS_2/ZIS	0.7576	51.52	2.8399	32.67	29.8186	15.81	23.7889

Table S5. Black experiments without catalyst nor light irradiation.[a]

Entry	Photocatalyst	Irradiation condition	Benzylamine conversion (%)	Imine yield (%)
1	10% ReS_2/ZIS	/	/	/
2	/	≥420 nm	/	/

[a] Reaction conditions: photocatalyst (10 mg), substrate (1 mmol), solvent 10 mL acetonitrile, room temperature, Xenon lamp ($\lambda \geq 420$ nm).

Table S6. Summary of photocatalysts reported for benzylamine oxidation.

Catalyst	Benzylamine amount (mmol)	Reaction time (h)	Solvent	TOF[a]	Reference
1%Pt/TiO_2-500 (50 mg)	1.074	12	H_2O+acetonitrile	0.974	Catal. Sci. Technol., 2019, 9, 5803
Polyhedral $SrTiO_3$ (4 mg)	0.4	16	acetonitrile	6.25	J. Mater. Chem. A, 2023, 11, 22198
COF-Sr2Fe1 (5 mg)	1.5	1.5	acetonitrile	19.4	J. Colloid Interface Sci. 2024, 655, 611
4-NA-Cu_2O (3 mg)	1	18	acetonitrile	18.2	ACS Catal. 2023, 13, 1474.
Titanium-Porphyrinic Aerogels (5 mg)	1	10	acetonitrile	20.00	Angew. Chem. Int. Ed., 2020, 59, 21591
$Bi_{24}O_{31}Br_{10}$ (20 mg)	0.2	12	H_2O	0.82	ChemSusChem, 2020, 13, 116
GICN (10 mg)	0.2	8	acetonitrile	2.33	Appl. Catal. B: Environ, 2020, 278, 119342
g-C_3N_4/BiOBr (100 mg)	0.125	4	acetonitrile	0.29	Chem. Eng. J., 2020, 394, 124934
Conjugated polyimide (50 mg)	0.1	6	acetonitrile	0.30	Appl. Catal. B: Environ, 2020, 272, 118964
CdS@C_3N_4 (5 mg)	0.3	4	acetonitrile	12.55	Appl. Catal. B: Environ, 2018, 236, 176
20% PDI/mpgCN (8 mg)	1	6	acetonitrile	20.63	Appl. Catal. B: Environ, **2021**, 298, 120534.
10% ReS_2/ZIS (10 mg)	**1**	**6**	**acetonitrile**	**22.84**	**This work**

[a] TOF: mmol of amine converted per gram of photocatalyst per hour.

References

1. G. Kresse, *J. Non-Cryst. Solids*, 1995, **192-193**, 222-229.
2. G. Kresse and J. Furthmuller, *Phys. Rev. B Condens. Matter.*, 1996, **54**, 11169-11186.
3. P. E. Blochl, *Phys. Rev. B Condens. Matter.*, 1994, **50**, 17953-17979.
4. G. Kresse and D. Joubert, *Phys. Rev. B*, 1999, **59**, 1758-1775.
5. J. P. Perdew, K. Burke and M. Ernzerhof, *Phys. Rev. Lett.*, 1996, **77**, 3865-3868.
6. S. Grimme, S. Ehrlich and L. Goerigk, *J. Comput. Chem.*, 2011, **32**, 1456-1465.
7. S. Grimme, J. Antony, S. Ehrlich and H. Krieg, *J. Chem. Phys.*, 2010, **132**, 154104.
8. M. Abdellah, K. Žídek, K. Zheng, P. Chábera, M.E. Messing and T. Pullerits, *J. Phys. Chem. Lett.*, 2013, **4,** 1760-1765.
9. X. Shi, M. Fujitsuka, S. Kim and T. Majima, *Small,* 2018, **14,** e1703277.
10. G. Yu, K. Gong, C. Xing, L. Hu, H. Huang, L. Gao, D. Wang and X. Li, *Chem. Eng. J.,* 2023, **461,** 142140.